© 2017. Published by The Company of Biologists Ltd | Development (2017) 144, 1887-1895 doi:10.1242/dev.143917

RESEARCH ARTICLE

Dominant-negative *Sox18* function inhibits dermal papilla maturation and differentiation in all murine hair types

Rehan Villani[1,2,*], Samantha Hodgson[1,*], Julien Legrand[1], Jessica Greaney[2], Ho Yi Wong[1], Cathy Pichol-Thievend[3], Christelle Adolphe[3], Brandon Wainwight[3], Mathias Francois[3] and Kiarash Khosrotehrani[1,2,‡]

ABSTRACT

SOX family proteins SOX2 and SOX18 have been reported as being essential in determining hair follicle type; however, the role they play during development remains unclear. Here, we demonstrate that *Sox18* regulates the normal differentiation of the dermal papilla of all hair types. In guard (primary) hair dermal condensate (DC) cells, we identified transient *Sox18* in addition to SOX2 expression at E14.5, which allowed fate tracing of primary DC cells until birth. Similarly, expression of *Sox18* was detected in the DC cells of secondary hairs at E16.5 and in tertiary hair at E18.5. Dominant-negative *Sox18* mutation (opposum) did not prevent DC formation in any hair type. However, it affected dermal papilla differentiation, restricting hair formation especially in secondary and tertiary hairs. This *Sox18* mutation also prevented neonatal dermal cells or dermal papilla spheres from inducing hair in regeneration assays. Microarray expression studies identified WNT5A and TNC as potential downstream effectors of SOX18 that are important for epidermal WNT signalling. In conclusion, SOX18 acts as a mesenchymal molecular switch necessary for the formation and function of the dermal papilla in all hair types.

KEY WORDS: Hair follicle, Dermal papilla, *Sox18*, Hair development

INTRODUCTION

Hair follicle (HF) development is a tightly regulated process that relies on interactions between the mesenchymal dermis and overlying epidermis. Hair development is characterised by the formation of a dermal condensate (DC) in response to epidermal signals (Millar, 2002). This DC then induces invagination of epidermal cells in hair placodes, which in turn pushes DC differentiation into the end-point lineage: the dermal papilla (DP). WNT, EDA/EDAR or hedgehog signalling are known to drive the specification of the epidermal component of the hair follicle, but far less is known about the molecular mechanisms that control the dermal differentiation process. WNT signalling has been implicated as being crucial for the first inductive signals for the DC; however, the mechanisms by which the DP develops from this is unknown.

[1]The University of Queensland, UQ Centre for Clinical Research, Royal Brisbane Hospital, Herston Road, Herston, Brisbane 4029, Queensland, Australia. [2]The University of Queensland, UQ Diamantina Institute, Translational Research Institute, 37 Kent Street, Woolloongabba, Brisbane 4102, Queensland, Australia. [3]The University of Queensland, Institute for Molecular Bioscience, 306 Carmody Road, St Lucia, Brisbane 4072, Queensland, Australia.
*These authors contributed equally to this work

‡Author for correspondence (k.khosrotehrani@uq.edu.au)

R.V., 0000-0001-8857-6271; M.F., 0000-0002-9846-6882; K.K., 0000-0002-6406-4076

Received 19 August 2016; Accepted 19 January 2017

Of significant interest, whereas HF development starts at E14.5, it occurs in three consecutive waves in mice, each giving rise to a different type of HF in dorsal epidermis: the first, starting at E14.5, gives rise to guard hairs; the second wave, at E16.5, gives rise to awl and auchene hairs; and the final wave, at E18.5, gives rise to zigzag hairs, the most abundant hair type in dorsal murine skin (Duverger and Morasso, 2009). Recent work in the field has suggested that the hair type could be determined by the DP. Identification of SOX2 as a specific DP marker and its restricted expression in guard, awl and auchene hairs prompted studies characterising its role at E14.5 in the DC of the first hair wave (Driskell et al., 2009). Unexpectedly, conditional ablation of *Sox2* in E14.5 DC allowed DPs and HFs to form. The resulting phenotype was modest and restricted to these three hair types (Clavel et al., 2012; Lesko et al., 2013). This suggests that expression of *Sox2* is dispensable for dermal papilla specification, even if it could be important for some aspects of its function. In particular, the ablation of *Sox2* had no effect on zigzag hairs (Graham et al., 2003).

DP cells that do not express *Sox2* have been shown to be enriched for *Sox18* (Driskell et al., 2009). *Sox18* is a member of the SOXF family of transcription factors that also includes *Sox17* and *Sox7* (Dunn et al., 1995). SOXF transcription factors modulate arteriovenous identity and lymphatic endothelial cell specification (Corada et al., 2013; Cermenati et al., 2008; Pendeville et al., 2008; Herpers et al., 2008; Francois et al., 2008). Murine models of *Sox18* mutation, including $Sox18^{-/-}$, $Sox18^{+/Ra}$ and $Sox18^{Op/+}$, have shown that *Sox18* also regulates hair follicle development (Carter and Phillips, 1954; Slee, 1962; Pennisi et al., 2000a,b; James et al., 2003). These studies report a defect that is restricted to zigzag hairs, supporting the view that SOX2 and SOX18 have complementing and non-overlapping functions that drive hair type formation (Slee, 1962; Pennisi et al., 2000a). More recent studies suggest *Sox2* and *Sox18* function in the dermal papilla, and Slee et. al. even suggest that *Sox18* may regulate DP development; however, it remains to be investigated how *Sox18* specifically regulates hair growth (Slee, 1962; Woo et al., 2012).

Importantly, in humans, mutation in *SOX18* has been reported to cause the human syndrome hypotrichosis-lymphedema-telangiectasia (HLT), a condition that manifests with hair loss, and lymphatic and cardiovascular defects (Irrthum et al., 2003). This condition is mimicked by $Sox18^{Op/+}$ mice, which harbour a dominant-negative mutation of *Sox18* ($Sox18^{Op/+}$) (James et al., 2003). This particular mutation suppresses the compensatory mechanisms by other SOX proteins observed in $Sox18^{-/-}$ mice (Hosking et al., 2009). The $Sox18^{Op/+}$ model is therefore particularly valuable for studying hair development and the role of SOX18 and SOXF in hair development and hair type specification.

In the present study, we report that the $Sox18^{Op/+}$ mutation results in abnormal hair follicle morphology of all hair types and we identify the SOXF factor *Sox18* as a crucial regulator of the DP differentiation program. We also demonstrate the importance of

Development (2017) 144, 1887-1895 doi:10.1242/dev.143917

Sox18-regulated WNT signalling interactions in all hair types between the mesenchymal DP and HF epithelium.

RESULTS

Sox18 is expressed in the dermal papilla of all HFs during development

We performed a comprehensive analysis of *Sox18* expression pattern, as determined by the activity of its endogenous regulatory elements during skin embryonic development (from E14.5 to E18.5) using a *Sox18*-GFP/CreER (*Sox18*$^{+/GFPCre}$) knock-in reporter mouse, which expresses GFP under the control of the endogenous *Sox18* promoter (Kartopawiro et al., 2014; McMahon et al., 2008). In the skin, expression of *Sox18*, as revealed by GFP detection, was restricted at all time-points to the DC structures, apart from some expected remnant expression in vascular structures. At E14.5, *Sox18* was expressed in the early DC (Fig. 1A, arrow). *Sox18* expression colocalised with the primary and secondary hair follicle marker SOX2, although its detection was not uniform within the DC (Driskell et al., 2009). The expression of *Sox18* in the primary HFs was short lived, as at E16.5 and E18.5, GFP could no longer be detected in the DC from primary HFs, which are identified by SOX2 expression. To determine whether all forming primary DC expressed *Sox18*, we performed whole-mount co-staining for SOX2 and GFP on E15.5 *Sox18*$^{+/GFPCre}$ embryos to identify GFP-positive DC. It appeared that all primary HFs were expressing *Sox18* within the SOX2-positive mesenchymal region (Fig. 1B). The expression of *Sox18* was also transiently detected in secondary follicle DC at E16.5, but not at E18.5 (Fig. 1C). Finally GFP (*Sox18*) was detected early in tertiary hair follicle development at E18.5 (Fig. 1C), where, as expected, tertiary hairs did not express SOX2 (Fig. 1C). We confirmed SOX18 protein expression at E18.5 using immunofluorescence co-staining with SOX2, which indicated that SOX18 protein expression could be detected in all hair follicle types (Fig. 1D) at E18.5, albeit at much lower levels in primary compared with secondary and tertiary HFs. To further confirm the expression of *Sox18* at E14.5 in primary follicles, we used lineage tracing by combining the *Sox18*$^{+/GFPCre}$ with an EYFP conditional reporter allele (+/*ROSA-EYFP*). By induction of Cre activity with tamoxifen at E14.5 in *Sox18*$^{+/GFPCre}$;+/*ROSA-EYFP* mice, we labelled cells derived from *Sox18*-expressing cells at E14.5 in primary HFs. We then detected, at birth, GFP/YFP expression via immunofluorescence and found that all visible cells within the DP of primary HFs were GFP/YFP+, along with the secondary and tertiary HFs, indicating overall *Sox18* was or is expressed in the DC of all hair waves (Fig. 1E). In addition, these lineage-tracing results confirmed that cumulatively all cells within each DC were labelled with YFP, indicating that, at one point in DC development, all cells express *Sox18*.

We next explored the expression of other SOXF family members, such as *Sox7*, using a *Sox7*-LacZ reporter mouse and SOX17 using immunofluorescence. At E14.5 and E16.5, neither *Sox7* (identified by β-galactosidase immunostaining) nor SOX17 could be identified in SOX2-expressing DC cells, although their presence was clearly

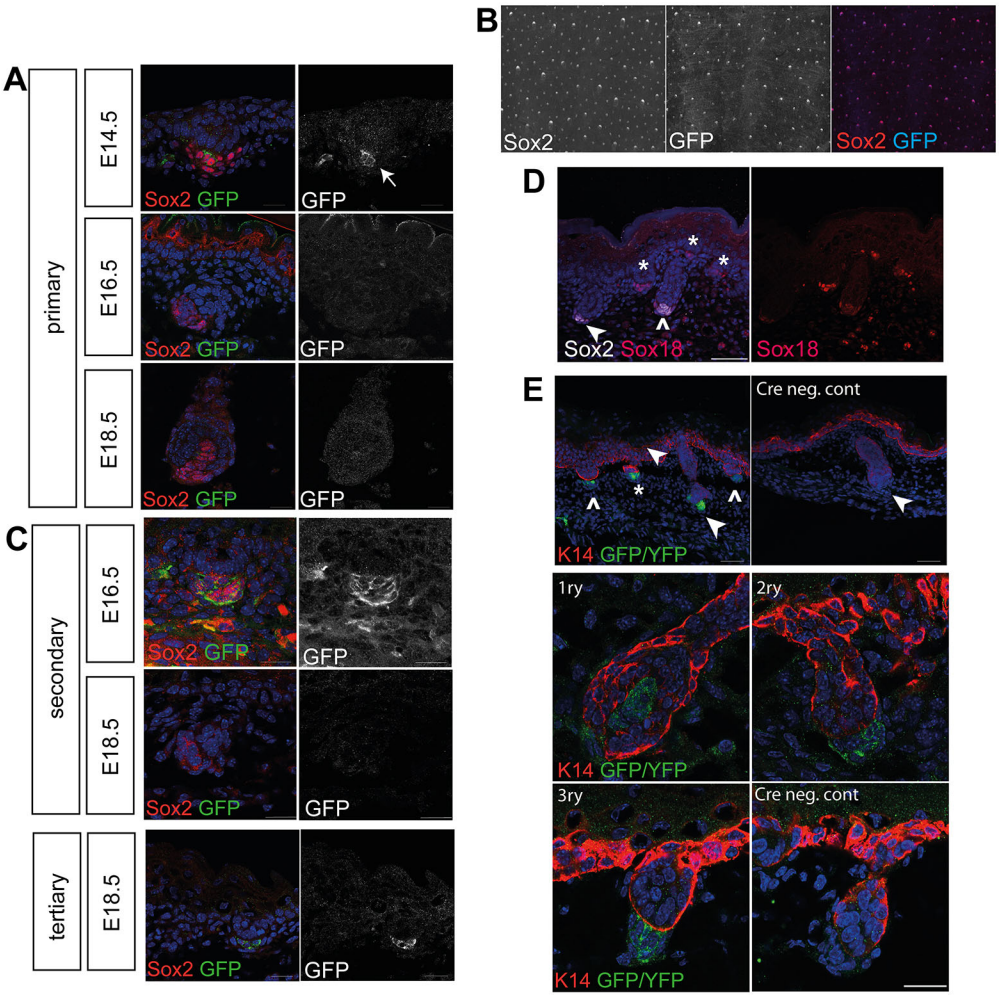

Fig. 1. Restricted temporal expression of *Sox18* in the mesenchymal component of all hair types. (A) Immunofluorescence detection of GFP (green), indicating SOX18, and SOX2 (red) in the dermal papilla of primary HFs at E14.5, E16.5 and E18.5 in *Sox18*$^{+/GFPCre}$ embryonic skin. (B) Whole-mount immunofluorescence confirms primary HF staining, showing overlap of SOX2 and SOX18 in the HFs at E15.5. (C) Immunofluorescence detection of GFP for SOX18 (green) and SOX2 (red) in the dermal papilla of secondary HFs at E16.5 and E18.5 in *Sox18*$^{+/GFPCre}$ embryonic skin. (D) SOX18 (red) and SOX2 (white) co-immunofluorescence at E18.5 in control C57bl/6 skin. (E) Lineage tracing of *Sox18*-expressing cells using anti-GFP/YFP staining at E18.5 of *Sox18*+/^{GFPCre};+/*ROSA-EYFP* (left) after *Sox18*-driven Cre expression by tamoxifen induction at E14.5 (on the left, negative control *Sox18*$^{+/+}$;+/*ROSA-EYFP*). Arrowhead indicates primary follicles, ^ indicates secondary follicles and asterisk indicates tertiary follicles. Scale bar: 50 µm (low magnification); 20 µm (high magnification). Negative controls indicated on panels are +/*ROSA-EYFP* (in absence of *Sox18*+/^{GFPCre} allele).

Development (2017) 144, 1887-1895 doi:10.1242/dev.143917

visible in surrounding vascular structures (Fig. S2A). Similarly, at E18.5, skin sections did not reveal any *Sox7* or SOX17 staining in primary, secondary or tertiary HFs (Fig. S2B). Overall, these data indicate the unique profile of expression of *Sox18* among SOXF family members in the mesenchymal component of developing HFs.

Dominant-negative *Sox18* affects HF development

Having established the mesenchymal expression pattern of *Sox18* using endogenous reporters during HF organogenesis, we next investigated its function. The human syndrome HLT and phenotypic analysis on mice carrying the dominant-negative $Sox18^{+/Op}$ mutation are characterised by alopecia; however, the molecular mechanism that underpins HF defects has yet to be elucidated (Irrthum et al., 2003; Pennisi et al., 2000b; Slee, 1962). Histological analysis of E14.5 $Sox18^{+/Op}$ epidermis revealed that primary HF induction was indistinguishable from that in control littermates (Fig. 2A). At E16.5, however, a delay in the further growth of primary follicles was evident and the placodes of secondary HFs were not easily detected. By the tertiary wave at E18.5, an even greater delay in hair development was observed and affected all hair types, despite clear formation of placodes (Fig. 2A). Similarly, at birth (P0), there was a marked difference between mutant and wild-type mice regarding outgrowth of secondary and tertiary HFs, whereas primary hair structures could still be observed, although delayed and abnormal. Quantification of hair follicle stage using the method described by Paus et al. at P0 further confirmed that, in $Sox18^{+/Op}$ mice, the majority of follicles were in an earlier phase of development compared with control (Paus et al., 1999).

Importantly, final hair formation, of all hair types, was abnormal in postnatal $Sox18^{+/Op}$ skin. Evaluation of the HF subtype in mutant mice and wild-type littermates clearly revealed a complete lack of zigzag and auchene hair in the $Sox18^{+/Op}$ mice (Fig. 2C, quantified in Fig. 2D), and compared with $Sox18^{-/-}$ mice (Pennisi et al., 2000a). The remaining hairs were either guard hairs or had a new hair phenotype somewhere between guard and awl hair types that could not easily be accurately classified. These hairs were larger, like guards; however, they contained a kink, like awls, although the kink was less marked than that of control awl hairs (Fig. 2C). These we quantified as awl hairs in Fig. 2D. We then showed, using histology, that, by P22, secondary and tertiary follicle development was totally disrupted, resulting in thin epithelial strands into the upper dermis (Fig. 2E). These hair remnants seemed to derive from

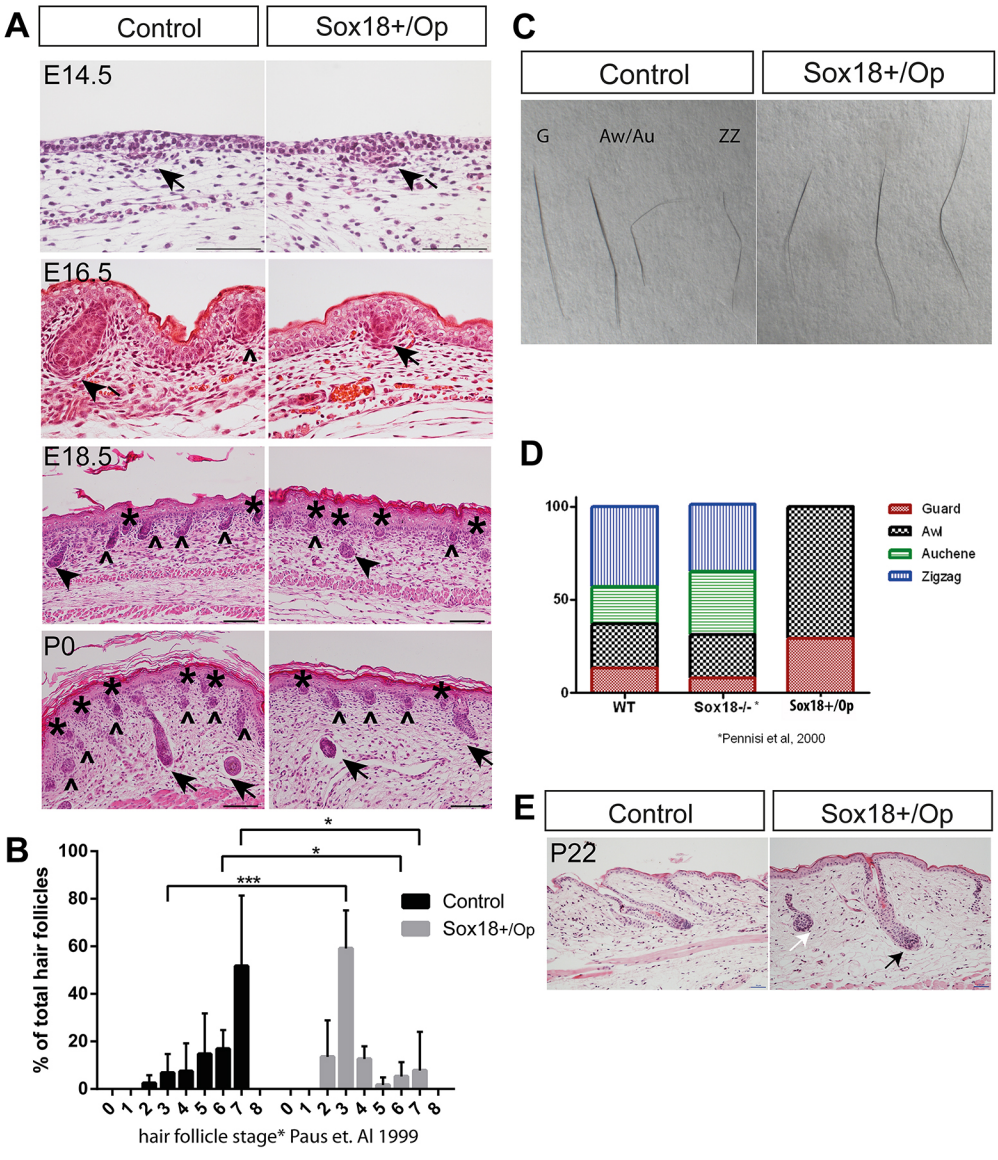

Fig. 2. HF development is delayed and hair-type ratios are altered in *Sox18*$^{+/OP}$ skin compared with littermate controls. (A) Haematoxylin and Eosin staining of control littermate and $Sox18^{+/Op}$ skin at E14.5, E16.5, E18.5 and P0. Black arrows indicate primary follicles, asterisks indicate secondary follicles and ^ indicates tertiary follicles. Scale bar: 100 µm. (B) Quantification in P0 skin of the percentage of hairs at each developmental stage (Paus et al., 1999); data are mean±s.e.m. **P*<0.05; ****P*<0.001. (C) Control and $Sox18^{+/Op}$ hair types, viewed at the same magnification. (D) Quantification of gross hair-type morphology in $Sox18^{+/Op}$ compared with control/wild-type skin and $Sox18^{-/-}$ mice (as reported by Pennisi et al., 2000a). (E) Haematoxylin and Eosin staining in P22 mice. Black arrow indicates guard hair; white arrow indicates hair remnant.

Development (2017) 144, 1887-1895 doi:10.1242/dev.143917

the secondary and tertiary hairs. Overall, these results indicate that a dominant-negative *Sox18*$^{+/Op}$ mutation affects HF development of all hairs, halting auchene and zigzag (and likely awl) hair development post-placode development and altering guard hairs.

Dominant-negative *Sox18* function disturbs guard HF development and cycling

Although we showed that *Sox18* is expressed in E14.5 DC cells, the *Sox18*$^{+/Op}$ mutation did not seem to prevent DP formation in primary hairs, which allowed their development. In order to determine whether guard HFs formed from the primary DP after *Sox18*$^{+/Op}$ mutation were normal, we explored their morphology and cycling. Interestingly, the remaining primary HFs, a much smaller proportion, also exhibited altered morphology and did not follow the parallel orientation observed in controls (Fig. 3A). When we compared guard hairs specifically (excluding the hairs that did not classify correctly as either guard or awl, mentioned earlier and Fig. 2C), the guard hair shafts obtained from plucking *Sox18*$^{+/Op}$ mice were also shorter (Fig. 3B). Furthermore, the hair density on the back skin was certainly decreased in *Sox18*$^{+/Op}$ skin (Fig. 3A). Histology showed that the remaining *Sox18*$^{+/Op}$ HFs had delayed entry into first catagen and telogen, as long HFs extending into the dermis were seen at all time-points, including P17 and P19 when normal skin displayed only catagen and telogen hairs (Fig. 3C). Ki67 staining further confirmed this, as proliferation could be seen in the hair matrix in the remaining *Sox18*$^{+/Op}$ guard hair, even at P19 (Fig. 3D).

To understand this alteration in cycling we next evaluated the effect of the *Sox18* mutation in the DP on the epidermal compartment. We first investigated hair differentiation using an AE13 antibody which showed that the differentiated inner root sheath was severely reduced in the remaining guard hairs in the *Sox18*$^{+/Op}$ mouse and completely absent from follicle remnants at P24 (Fig. S2), potentially explaining the reduced size of the hair shaft. We then analysed epidermal progenitor cell markers: SOX9 staining indicated that mutant mice maintained a proliferative progenitor compartment comparable with controls (Vidal et al., 2005). NFATc1 and CD34, markers of dormant epidermal bulge stem cells, appeared significantly reduced in *Sox18*$^{+/Op}$ compared with control follicles (Fig. S2B-D). The loss of this cell population combined with the observed hyperproliferation and lack of telogen stage suggested an excessive activation of HF stem cells. This led to a permanently maintained anagen phase that resulted in their exhaustion at later stages. In support of this hypothesis, 12-month-old *Sox18*$^{+/Op}$ mice showed a total loss of hair shafts and few hair remnants were still observed that did not stain for *Sox9* (Fig. S2E-F). In summary, dominant-negative mutation of *Sox18* in secondary and tertiary follicles results in complete loss of all hair markers; in primary (or guard) hairs, it resulted in decreased hair stem cell markers and reduced hair differentiation.

Sox18 function is cell-autonomous in dermal mesenchymal cells during hair regeneration

In order to determine the compartmental origin of the HF defect in *Sox18*$^{+/Op}$ in either epidermal or mesenchymal skin, we employed hair regeneration assays. Wild-type or *Sox18*$^{+/Op}$ mutant neonatal dermis and keratinocytes were mixed in multiple combinations to assess HF regeneration (Fig. 4). Wild-type keratinocytes combined with wild-type dermis resulted in significant hair regeneration 2 weeks post-injection (Fig. 4A), whereas a combination of *Sox18*$^{+/Op}$ keratinocytes and *Sox18*$^{+/Op}$ dermis recapitulated the *Sox18*$^{+/Op}$ phenotype of greatly decreased hair formation (Fig. 4B). Interestingly, *Sox18*$^{+/Op}$ dermis combined with wild-type

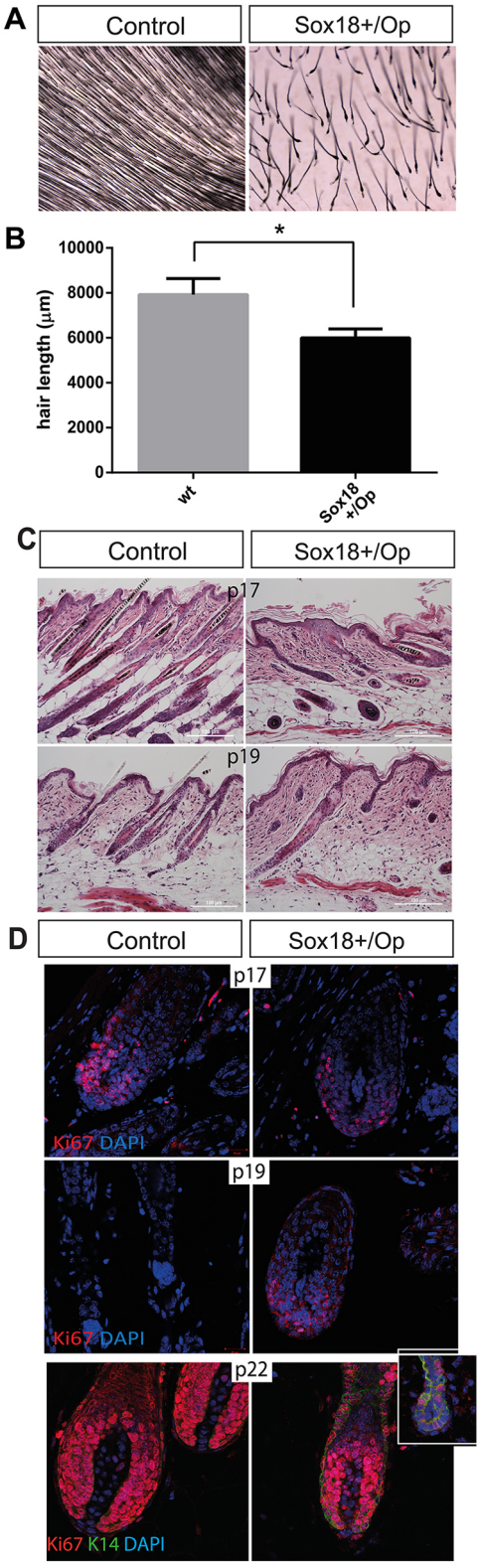

Fig. 3. *Sox18*$^{+/Op}$ guard hairs exhibit constant proliferation and altered hair cycle. (A) Whole-mount visualisation of control and *Sox18*$^{+/Op}$ skin, identifying differences in hair shaft density and orientation in the skin. (B) Quantification of hair length of control and *Sox18*$^{+/Op}$ hairs (data are mean±s.e.m.; control, n=3; *Sox18*$^{+/Op}$, n=3, *P<0.05). (C) Haematoxylin and Eosin staining of control littermate and *Sox18*$^{+/Op}$ skin at P17 and P19. (D) Immunodetection of Ki67 (red), DAPI counterstain (blue) in control and *Sox18*$^{+/Op}$ skin at P17, P19 and P22. Inset displays Ki67 staining in a hair remnant.

Development (2017) 144, 1887-1895 doi:10.1242/dev.143917

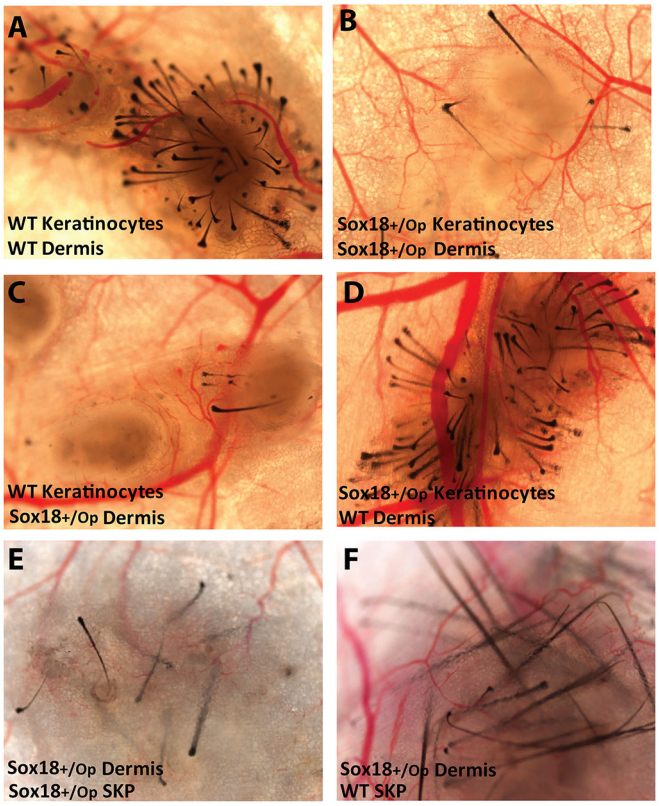

Fig. 4. Wild-type dermal-derived spheroids (SKPs) rescue hair regeneration assays using *Sox18*$^{+/OP}$ cells. Photomicrograph of whole-mount subcutaneous view of patches obtained in hair regeneration assays by subcutaneous injection of different cell populations. (A) Patch assay performed by combining neonatal wild-type keratinocytes and wild-type dermis. (B) Patch assay performed with neonatal *Sox18*$^{+/OP}$ keratinocytes and *Sox18*$^{+/OP}$ dermis. (C) Patch assay performed with wild-type keratinocytes and *Sox18*$^{+/OP}$ dermis. (D) Patch assay performed with *Sox18*$^{+/OP}$ keratinocytes and wild-type dermis. (E) Patch assay performed with *Sox18*$^{+/OP}$ dermis and keratinocytes, with the addition of *Sox18*$^{+/OP}$ dermal-derived SKPs. (F) Patch assay performed with *Sox18*$^{+/OP}$ dermis and keratinocytes with addition of wild-type-derived SKPs. Images are representative of three independent experiments.

keratinocytes (Fig. 4C) could not induce hair regeneration to anywhere near the same extent as wild-type dermis combined with either wild-type or *Sox18*$^{+/Op}$ keratinocytes (Fig. 4A,D). These data suggest the *Sox18*$^{+/Op}$ defect was of dermal origin.

We next developed neonatal dermal-derived spheres, adopting the skin-derived precursor (SKP) culture method for both wild-type and *Sox18*$^{+/Op}$ mutant mice (Biernaskie et al., 2007). SKPs were easily produced from neonatal dermis and unanimously expressed SOX2 and *Sox18* (Fig. S4). SKPs from *Sox18*$^{Op/+}$ mice did not change the phenotype observed in hair regeneration assays when added to *Sox18*$^{Op/+}$ dermis and keratinocytes (Fig. 4E). However, wild-type dermal-derived SKPs increased the number of hairs regenerated in the same assay mixing mutant dermis and keratinocytes (n=3) (Fig. 4F). This indicates that wild-type dermal SKPs have intrinsic *Sox18*-dependent properties that can rescue HF formation inhibited by dominant-negative *Sox18* mutation in the dermal component.

Sox18 loss of function inhibits dermal papilla formation but not its specification

In accordance with our initial findings of *Sox18* expression in the DC, we sought to determine whether the *Sox18* mutation was affecting DC specification. Interestingly, secondary and tertiary hair remnants showed inhibited DC differentiation, as very little alkaline phosphatase and no CD133 staining could be identified at P0 in the extremity of invaginating epithelial structures (Fig. 5A,B). Similarly, no α-smooth muscle actin could be identified in the mesenchyme surrounding each follicle (Fig. 5C). Specification of DC and DP was occurring, indicated by SOX2, which marks primary and secondary follicle DC cells (Fig. S1) and LEF1

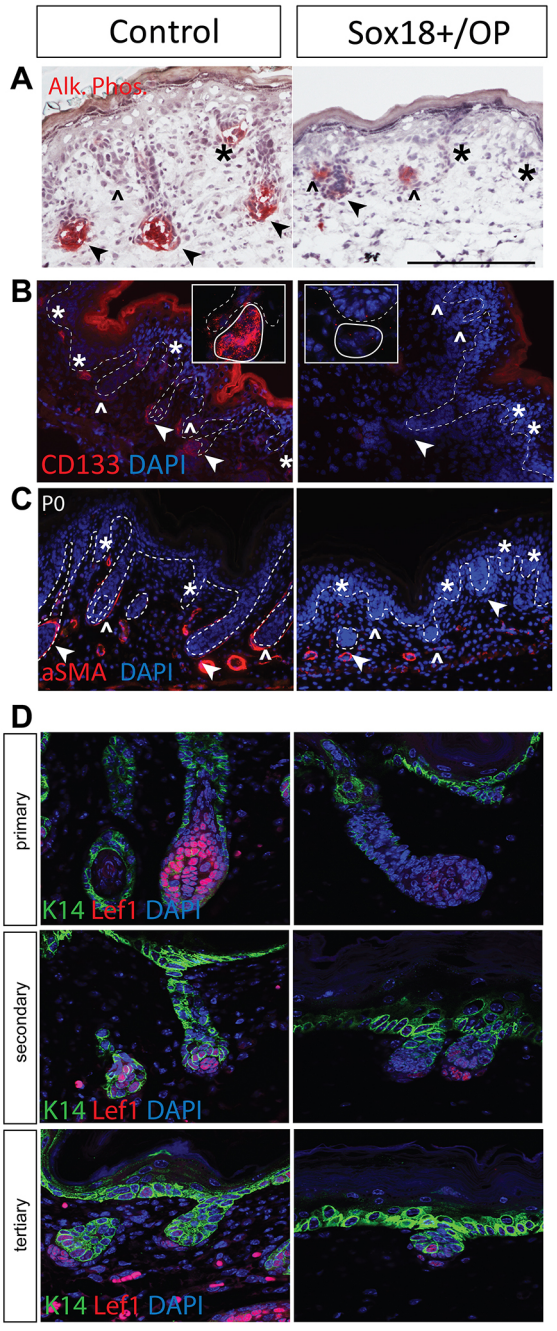

Fig. 5. Dermal papilla differentiation is inhibited in *Sox18*$^{+/OP}$ skin. Immunofluorescence staining of skin sections from *Sox18*$^{+/OP}$ and wild-type littermate controls. (A) Alkaline phosphatase staining (blue). (B) CD133 (red) stains the DP in control P0 skin. (C) α-smooth muscle actin (red) stains the DP and the dermal sheath in addition to pericytes in P0 skin. Arrow indicates primary follicles, ^ indicates secondary follicles and asterisk indicates tertiary follicles. (D) LEF1 (red) expression in developing hairs; keratin 14 expression (green) indicates the epidermal-expressing cells at P0 in control and *Sox18*$^{+/OP}$ skin.

Development (2017) 144, 1887-1895 doi:10.1242/dev.143917

(Fig. 5D), which, although not specific to the DC, is expressed in all hair types. We showed that the WNT signalling responsible for DC specification was induced because LEF1, a downstream target of WNT, could be detected in the condensate of developing HFs at all stages (Fig. 5D). These findings indicate that the dominant-negative defect of SOX18 allowed formation of a mesenchymal condensate with LEF1 expression. However, this DC failed to differentiate into a dermal papilla and to generate the second dermal signal for HF development.

Gene expression analysis identifies regulation of WNT signal modulators in *Sox18* dominant-negative mutant dermal spheres

In order to better understand how dominant-negative *Sox18* mutation is affecting the DP, we performed gene expression microarray on dermal spheres (SKPs) isolated from $Sox18^{+/Op}$ and wild-type littermate neonates that demonstrated differential hair inductive capacity. Comparisons were made within the same litter and animals were matched for sex. Unsupervised clustering analysis classified samples according to their genotype (Fig. S4). 2570 genes were differentially expressed with a *P*-value less than 0.05 after correction for multiple testing. Among these, 576 showed over twofold differences between control and $Sox18^{+/OP}$ SKPs. Among the dysregulated genes, *Wnt5a* (2.4 fold, $P<0.05$), *Fgf7* (2.2 fold, $P=0.014$), *Wnt7b* (2.2 fold, $P<0.05$), *Mmp9* (18 fold, $P<0.05$) and *Tnc* (1.8 fold, $P<0.01$), all known as important contributors to the regulation of hair cycling or hair development by the DP, were significantly downregulated in $Sox18^{+/OP}$ mutants. Other genes, such as *Epha7* (a known target of SOX18) were also downregulated (2.4-fold, $P<0.05$) (Hoeth et al., 2012). WNT5A, MMP9 and TNC downregulation was confirmed by real-time PCR in $Sox18^{+/OP}$ compared with control dermal spheres (Fig. 6A). Furthermore, WNT5A and TNC immunofluorescence showed a significant reduction of expression in the $Sox18^{+/OP}$ skin, in part explaining the observed phenotype (Fig. 6B,C) (Youssef et al., 2012; Kaplan and Holbrook, 1994).

Altered dermal WNT ligands and modulators result in decreased epidermal WNT signalling in *Sox18* dominant-negative mutants

WNT5A and TNCC have been previously implicated as regulators of WNT signalling in hair and whisker (Reddy et al., 2001; Hendaoui et al., 2014). To determine how the secreted factors WNT5A and TNC may be affecting WNT signalling in the skin, we crossed $Sox18^{+/Op}$ mice with a Flash reporter line expressing luciferase in cells with active canonical WNT signalling (Hodgson et al., 2014). WNT signalling was reduced in $Sox18^{+/Op}$ mice compared with controls globally, at all phases of the hair cycle. Luminescence analysis in $Sox18^{+/Op}$:$Flash^{+/-}$ mice indicated that the WNT signalling was at a baseline activity that did not strongly cycle (Fig. 7A,B). Interestingly, these data also supported our findings of delayed hair development and cycling in $Sox18^{+/Op}$ mice (Fig. 3). However, as global WNT signalling decrease may reflect the lower density of hair follicles, we also investigated at the individual follicle level. LEF1 immunofluorescence performed on P24 skin further supported that the remaining WNT signalling from the epidermal compartment was reduced in intensity in $Sox18^{+/Op}$ mice (Fig. 7C). This was further confirmed by β-catenin immunofluorescence. Nuclear staining, specifically in the epidermal compartment, of hair follicles confirmed fewer cells with active WNT signalling in $Sox18^{+/Op}$ hair follicles when compared with control (Fig. 7D).

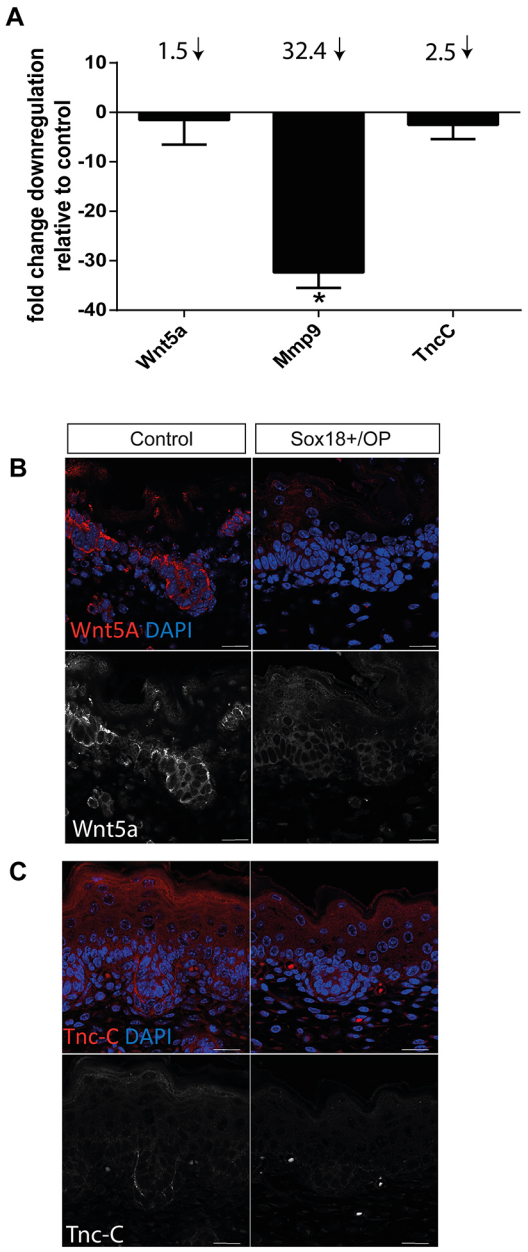

Fig. 6. Expression array identifies genes affected by *Sox18* loss of function. (A) Real-time PCR on cDNA from dermal SKPs for *Wnt5a* (control, $n=5$; $Sox18^{+/OP}$, $n=5$), *Mmp9* (control, $n=6$; $Sox18^{+/OP}$, $n=6$) and *Tncc* (control, $n=5$; $Sox18^{+/Op}$, $n=3$) as genes regulated by *Sox18* activity. (B) WNT5A (red) immunostaining in E18.5 control and $Sox18^{+/OP}$ skin. (C) Tenascin C (Tnc-C, red) immunostaining in E18.5 control and $Sox18^{+/OP}$ skin. Scale bars: 20 µm. Error bars indicate s.e.m.

DISCUSSION

The molecular events leading to the development and function of the dermal clusters and dermal papillae remain unclear. Here, we have identified the essential role of *Sox18* in DP development and function, especially in secondary and tertiary hairs but also in primary hairs. Indeed, *Sox18* was expressed in a highly temporally restricted manner in the developing DP of all HF types. The absence of other SOXF family members in the DC of dorsal skin further supported the important role of *Sox18* in this process. Dominant-negative mutation of *Sox18* inhibited DP formation and differentiation without affecting early stages of dermal condensation. Skin-derived precursor (SKP)

Development (2017) 144, 1887-1895 doi:10.1242/dev.143917

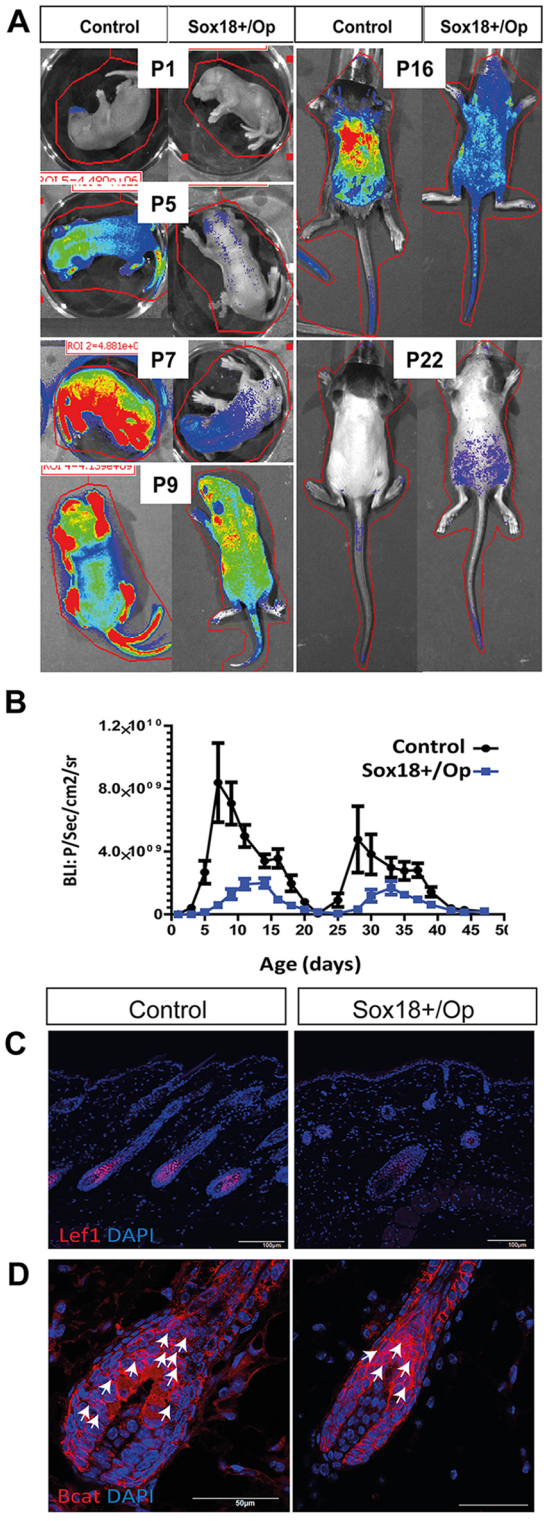

Fig. 7. *Sox18* dominant-negative mutation leads to alterations in WNT signalling. (A) *Sox18*$^{+/Op}$*:Flash*$^{+/-}$ and *Flash*$^{+/-}$ control mice were injected with luciferin at P1, P5, P7, P9, P16 and P22 and imaged for bioluminescence. (B) Quantification of bioluminescence over time post birth (*n*=22, control; *n*=23, *Sox18*$^{+/Op}$; data are mean±s.e.m.). (C) LEF1 immunostaining showed LEF1 staining in the hair matrix and dermal papilla during early anagen at P24 in *Flash*$^{+/-}$ control mice; however, in *Sox18*$^{+/Op}$*:Flash*$^{+/-}$ mice, LEF1 is only detectable in guard hairs and only in the epidermal matrix compartment. Scale bars: 100 µm. (D) β-Catenin immunofluorescence in the *Sox18*$^{+/Op}$ and control hair follicle matrix and DP at P22. Arrows indicate β-catenin-positive nuclei, identified by overlap with DAPI stain. Scale bars: 50 µm.

dermal spheres from wild-type mice restored the *Sox18*$^{+/Op}$ phenotype in hair regeneration assays, further demonstrating that the defect in *Sox18*$^{+/Op}$ mice is dermal and that *Sox18* function is cell-autonomous. Finally, gene expression arrays using skin-derived precursor (SKP) dermal spheres, identified WNT5A and TNC as a potential downstream effectors of *Sox18* in the dermal papilla that we hypothesise are mediating decreases in WNT signalling in the neighbouring epidermal HF cells.

A first contradiction that motivated this study was the proposed role of *Sox18* in only zigzag hairs, which is opposed to its reported expression in the DC at E14.5 in a single study (Pennisi et al., 2000a). *Sox18* reporter activity, SOX18 immunofluorescence and lineage tracing undoubtedly indicate that *Sox18* is expressed at the RNA level in the mesenchymal component of all HFs limited to stages 1-2 of HF development (Paus et al., 1999), but persists at protein level beyond this stage until birth. When the follicle developed beyond stage 3, when the DP is engulfed by the epidermal matrix, *Sox18* expression could no longer be detected in primary or secondary follicles. Despite the GFP reporter expression in *Sox18*$^{+/GFPCre}$ only labelling some DP cells, lineage tracing showed that all cells within each dermal cluster express SOX18, indicating that all DP cells express *Sox18* at one point within their development.

The inhibition of hair development in *Sox18*$^{+/Op}$ skin supports that SOX18/SOXF are required for the normal formation of the DP. The phenotype observed in *Sox18*$^{+/Op}$ mutant mice is much more severe compared with previous reports of *Sox18*$^{-/-}$ mice (Pennisi et al., 2000a). Previous studies focusing on the cardiovascular phenotype of these same mice have reported a possible compensatory mechanism by other SOXF factors, notably SOX17 when SOX18 is fully lost (Hosking et al., 2009). By contrast, the *Sox18*$^{+/Op}$ mutation, a single-point cytosine mutation at residue 1048, creates a missense transcript and a truncated version of the protein that prevent this transcription factor from recruiting normal SOX18 or its interacting partner MEF2C (James et al., 2003). The *Sox18*$^{+/Op}$ mutation results in dominant-negative activity of SOX18 that abrogates its own activity as well as the role of its binding partners. Although we could not find SOX17 or *Sox7* in the DC/DP during hair development, other SOX proteins, such as SOX2 or other binding partners could be involved in the observed phenotype of *Sox18*$^{+/Op}$ mutation. As such, given the wide expression of *Sox18*, the *Sox18*$^{+/Op}$ phenotype observed here highlights the activity of the complex formed by SOX18 with its binding partners rather than the activity of SOX18 alone. However, an important partner of this transcription factor complex is SOX18 itself.

The epidermis was not affected by the *Sox18*$^{+/Op}$ mutation as it could be induced to form HFs. Moreover, SOX2 expression was normally detected in primary and secondary DC cells of mice with *Sox18*$^{+/Op}$. This suggested that DC formation and the first 'inductive' dermal signal was independent of SOX18 activity. Rapidly, after DC formation in *Sox18*$^{+/Op}$ mice at all stages, there was a defect in epidermal invagination and proliferation, suggesting that the second dermal signal inducing HF growth was absent. Our gene expression array and further validation identified WNT5A as a potential candidate 'second signal' affected by *Sox18* mutation that might be necessary for hair development. In addition, *Sox18*$^{Op/+}$ skin did not display normal DP formation, as witnessed by the loss of CD133, α-smooth muscle actin and alkaline phosphatase activity, the most commonly used markers of differentiated DP and dermal sheath. When combined, these data suggest that, after DC induction, SOX18, despite its restricted expression in time, allows for the differentiation of function of DP cells and their hair inductive properties.

Development (2017) 144, 1887-1895 doi:10.1242/dev.143917

The presence of dominant-negative SOX18 at E14.5 in primary DC cells had long-term consequences, despite the expression of SOX2 resulting in a loss of quiescent epidermal stem cells, extended anagen periods, poor differentiation (likely due to reduced number of cells with active WNT signalling) and long-term exhaustion of epidermal stem cells. These indirect effects on the epidermis in guard hairs further highlight the importance of SOX18 and its binding partners in the long-term regulatory function of the dermal papilla. This also implies that *Sox18* might have different functions in guard versus awl/auchene/zigzag hairs. This may be related to stronger activity of its interaction partners in guard and awl hairs. SOX2 is an obvious candidate for interaction with SOX18 and this role remains to be established. This is reminiscent of observations in the equivalent human disease HLT that occurs through homozygous or dominant-negative SOX18 mutation (Irrthum et al., 2003). Indeed, individuals with HLT are born with no eyebrows or eyelashes, and never develop any pubic or axillary hair at puberty. However, they have some scalp hair that is rapidly lost within the first few months to years after birth.

In summary, *Sox18* expression is spatiotemporally regulated and detected in the mesenchymal component of all developing hair types. Its function in association with its binding partners is required to mediate DP differentiation and promotion of epidermal changes that will form the hair, possibly through production of WNT ligands and modulators. SOX18 activity in combination with its binding partners at E14.5 is further needed for proper regulation of quiescence and cycling of guard hair epidermal stem cells. These findings further elucidate the development of the dermal papilla, as well as the mechanism of the human HLT syndrome. This will aid the identification of the molecular cues in the dermal component that lead to the development of HFs.

MATERIALS AND METHODS

Mouse models

+/Sox18GCre mice were kindly provided by Dr Andy McMahon (Kartopawiro et al., 2014; McMahon et al., 2008). *Sox18*$^{+/Op}$ mice were obtained from Prof. Peter Koopman (Institute for Molecular Bioscience, The University of Queensland, Australia) and +/Flash reporter mice were as described previously (Hodgson et al., 2014). *Sox7-LacZ* knock-in mice were generated using Velocigene targeting of *Sox7* gene using a BAC clone with a LacZ insert (Regeneron, Tarrytown, NY, USA). These mice were kindly provided by Dr Nicolas Fossat. All murine work was performed to institutional ethical requirements (University of Queensland Animal Ethics Committee).

Histology/Immunofluorescence

Primary antibodies used on frozen tissue were SOX2 (1/100, Abcam ab97959, lot#196138-7), GFP (1/100, Life Technologies A10262, lot#1729643), CD34 MEC 14.7 (1/50, Abcam ab8158) and CD133 (1/50, Ebioscience 14-1331-80, lot#E04033-1631). Primary antibodies used on paraffin wax-embedded tissue were LEF1 C12 A5 (1/150, Cell Signalling CST2230), CD26 H194-112 (1/50, R&D AF954), Dlk (1/50, Abcam ab21682, lot#GR192235-1), αSMA 1A4 (1/100, Abcam ab7187), anti-hair cytokeratin AE13 (1/500, Abcam ab16113), SOX9 H-90 (1/200, Santa Cruz sc20095), Nfatc1 7-A6 (1/100, Santa Cruz sc7294), SOX18 H-140 (1/50, Santa Cruz sc20100) and WNT5A 3D10 (1/100, Abcam ab86720). Secondary antibodies used were anti-rabbit A568, anti-rabbit A488, anti-goat A488 and anti-chicken A647 (Invitrogen), all used at 1/500 dilution. Immunofluorescence was performed on both 4% paraformaldehyde (PFA) paraffin wax-embedded skin or 1% PFA-fixed cryoembedded skin; all sections were counterstained with DAPI. Images were acquired on either a Zeiss LSM 710 or Olympus FV1200 confocal microscope.

Luciferase analysis

Luciferase analyses were performed as previously described (Hodgson et al., 2014). Briefly, mice were injected with 150 mg/kg D-Luciferin Firefly (Caliper) and imaged after 10 min using a Xenogen IVIS Spectrum live animal imaging system. Analysis was performed using Living Image Software.

Microarray

Microarray experiments were performed on n=3 control and n=3 *Sox18*$^{+/Op}$ sex-matched littermate SKP samples. Preparation and analysis was performed as previously established (Rodero et al., 2013).

RT-PCR

RNA was isolated from ∼1×10^6 SKP cells, separated by dispase digestion for 2 h at 37°C, using a Qiagen RNeasy kit. RNA (1 µg) was used for cDNA preparation using superscript III, according to the manufacturer's instructions. RT-PCR was performed using SYBR Green (Applied Biosystems) on a StepOne Plus real-time PCR machine (Applied Biosystems). Ct values were exported and data analysed using Excel and GraphPad Prism. Statistical significance was determined using an unpaired t-test between the relative RNA species amounts in control and *Sox18*$^{+/OP}$ samples. Data represent the fold change.

Hair regeneration assay

Dermal and epidermal cells were prepared after skin was removed from neonate mice, washed in antibacterial and anti-mycotic solutions. Epidermis was separated overnight in Dispase II (Sigma Aldrich) (5 mg/ml at 4°C). Epidermal sheets were then incubated on TrypLE (Gibco) for 20 min at room temperature and epidermal cells pelleted. For each patch assay, between 1×10^6 and 2×10^6 dermal cells and 1×10^6 epidermal cells were injected subcutaneously in nude mice. Patch assays were analysed after 2 weeks.

Hair analyses

Hair development was analysed by counting number of hairs at each hair development phase using Haematoxylin/Eosin-stained tissue (Paus et al., 1999). Hair type and length was quantified from the plucked back skin of 3-week-old wild-type and *Sox18*$^{+/OP}$ littermates observed using light microscopy. Type counts were then averaged and compared with previously reported values (Pennisi et al., 2000a). Statistical tests performed were Student t-test on both hair stage (Fig. 2) and hair length (Fig. 3).

Acknowledgements

We thank Patrick Tam, Nicolas Fossat and Tania Radziewic (CMRI, UNSW, Sydney) for the kind gift of the Sox7-LacZ mouse line. We thank Peter Koopman and Andy McMahon for access mouse lines.

Competing interests

The authors declare no competing or financial interests.

Author contributions

K.K., R.V., M.F., S.H., C.A. and B.W. designed experiments and analysed data. R.V., S.H., J.L., J.G., C.P.-T. and H.Y.W. performed experiments. All authors contributed to manuscript writing and proofreading.

Funding

This work was supported by a Career Development Fellowship from the Australian National Health and Medical Research Council (to K.K.) and an Australian Research Council Discovery Project grant (DP130104777).

Data availability

Microarray data are available in the ArrayExpress database under accession number E-MTAB-5673 (https://www.ebi.ac.uk/arrayexpress/experiments/E-MTAB-5673/).

Supplementary information

Supplementary information available online at
http://dev.biologists.org/lookup/doi/10.1242/dev.143917.supplemental

References

Biernaskie, J., Sparling, J. S., Liu, J., Shannon, C. P., Plemel, J. R., Xie, Y., Miller, F. D. and Tetzlaff, W. (2007). Skin-derived precursors generate myelinating Schwann cells that promote remyelination and functional recovery after contusion spinal cord injury. *J. Neurosci.* **27**, 9545-9559.

Carter, T. C. and Phillips, R. J. S. (1954). Ragged, a semidominant coat texture mutant - in the house mouse. *J. Hered.* **45**, 150-154.

Development (2017) 144, 1887-1895 doi:10.1242/dev.143917

Cermenati, S., Moleri, S., Cimbro, S., Corti, P., Del Giacco, L., Amodeo, R., Dejana, E., Koopman, P., Cotelli, F. and Beltrame, M. (2008). Sox18 and Sox7 play redundant roles in vascular development. *Blood* **111**, 2657-2666.

Clavel, C., Grisanti, L., Zemla, R., Rezza, A., Barros, R., Sennett, R., Mazloom, A. R., Chung, C.-Y., Cai, X., Cai, C.-L. et al. (2012). Sox2 in the dermal papilla niche controls hair growth by fine-tuning BMP signaling in differentiating hair shaft progenitors. *Dev. Cell* **23**, 981-994.

Corada, M., Orsenigo, F., Morini, M. F., Pitulescu, M. E., Bhat, G., Nyqvist, D., Breviario, F., Conti, V., Briot, A., Iruela-Arispe, M. L. et al. (2013). Sox17 is indispensable for acquisition and maintenance of arterial identity. *Nat. Commun.* **4**, 2609.

Driskell, R. R., Giangreco, A., Jensen, K. B., Mulder, K. W. and Watt, F. M. (2009). Sox2-positive dermal papilla cells specify hair follicle type in mammalian epidermis. *Development* **136**, 2815-2823.

Dunn, T. L., Mynett-Johnson, L., Wright, E. M., Hosking, B. M., Koopman, P. A. and Muscat, G. E. O. (1995). Sequence and expression of Sox-18 encoding a new HMG-box transcription factor. *Gene* **161**, 223-225.

Duverger, O. and Morasso, M. I. (2009). Epidermal patterning and induction of different hair types during mouse embryonic development. *Birth Defects Res. C Embryo Today* **87**, 263-272.

Francois, M., Caprini, A., Hosking, B., Orsenigo, F., Wilhelm, D., Browne, C., Paavonen, K., Karnezis, T., Shayan, R., Downes, M. et al. (2008). Sox18 induces development of the lymphatic vasculature in mice. *Nature* **456**, 643-647.

Graham, V., Khudyakov, J., Ellis, P. and Pevny, L. (2003). SOX2 functions to maintain neural progenitor identity. *Neuron* **39**, 749-765.

Hendaoui, I., Tucker, R. P., Zingg, D., Bichet, S., Schittny, J. and Chiquet-Ehrismann, R. (2014). Tenascin-C is required for normal Wnt/beta-catenin signaling in the whisker follicle stem cell niche. *Matrix. Biol.* **40**, 46-53.

Herpers, R., Van de Kamp, E., Duckers, H. J. and Schulte-Merker, S. (2008). Redundant roles for sox7 and sox18 in arteriovenous specification in zebrafish. *Circ. Res.* **102**, 12-15.

Hodgson, S. S., Neufeld, Z., Villani, R. M., Roy, E. and Khosrotehrani, K. (2014). Transgenic flash mice for in vivo quantitative monitoring of canonical Wnt signaling to track hair follicle cycle dynamics. *J. Invest. Dermatol.* **134**, 1519-1526.

Hoeth, M., Niederleithner, H., Hofer-Warbinek, R., Bilban, M., Mayer, H., Resch, U., Lemberger, C., Wagner, O., Hofer, E., Petzelbauer, P. et al. (2012). The transcription factor SOX18 regulates the expression of matrix metalloproteinase 7 and guidance molecules in human endothelial cells. *PLoS ONE* **7**, e30982.

Hosking, B., Francois, M., Wilhelm, D., Orsenigo, F., Caprini, A., Svingen, T., Tutt, D., Davidson, T., Browne, C., Dejana, E. et al. (2009). Sox7 and Sox17 are strain-specific modifiers of the lymphangiogenic defects caused by Sox18 dysfunction in mice. *Development* **136**, 2385-2391.

Irrthum, A., Devriendt, K., Chitayat, D., Matthijs, G., Glade, C., Steijlen, P. M., Fryns, J.-P., Van Steensel, M. A. M. and Vikkula, M. (2003). Mutations in the transcription factor gene SOX18 underlie recessive and dominant forms of hypotrichosis-lymphedema-telangiectasia. *Am. J. Hum. Genet.* **72**, 1470-1478.

James, K., Hosking, B., Gardner, J., Muscat, G. E. O. and Koopman, P. (2003). Sox18 mutations in the ragged mouse alleles ragged-like and opossum. *Genesis* **36**, 1-6.

Kaplan, E. D. and Holbrook, K. A. (1994). Dynamic expression patterns of tenascin, proteoglycans, and cell adhesion molecules during human hair follicle morphogenesis. *Dev. Dyn.* **199**, 141-155.

Kartopawiro, J., Bower, N. I., Karnezis, T., Kazenwadel, J., Betterman, K. L., Lesieur, E., Koltowska, K., Astin, J., Crosier, P., Vermeren, S. et al. (2014). Arap3 is dysregulated in a mouse model of hypotrichosis-lymphedema-telangiectasia and regulates lymphatic vascular development. *Hum. Mol. Genet.* **23**, 1286-1297.

Lesko, M. H., Driskell, R. R., Kretzschmar, K., Goldie, S. J. and Watt, F. M. (2013). Sox2 modulates the function of two distinct cell lineages in mouse skin. *Dev. Biol.* **382**, 15-26.

McMahon, A. P., Aronow, B. J., Davidson, D. R., Davies, J. A., Gaido, K. W., Grimmond, S., Lessard, J. L., Little, M. H., Potter, S. S., Wilder, E. L. et al. (2008). GUDMAP: the genitourinary developmental molecular anatomy project. *J. Am. Soc. Nephrol.* **19**, 667-671.

Millar, S. E. (2002). Molecular mechanisms regulating hair follicle development. *J. Invest. Dermatol.* **118**, 216-225.

Paus, R., Müller-Röver, S., van der Veen, C., Maurer, M., Eichmuller, S., Ling, G., Hofmann, U., Foitzik, K., Mecklenburg, L. and Handjiski, B. (1999). A comprehensive guide for the recognition and classification of distinct stages of hair follicle morphogenesis. *J. Invest. Dermatol.* **113**, 523-532.

Pendeville, H., Winandy, M., Manfroid, I., Nivelles, O., Motte, P., Pasque, V., Peers, B., Struman, I., Martial, J. A. and Voz, M. L. (2008). Zebrafish Sox7 and Sox18 function together to control arterial-venous identity. *Dev. Biol.* **317**, 405-416.

Pennisi, D., Bowles, J., Nagy, A., Muscat, G. and Koopman, P. (2000a). Mice null for sox18 are viable and display a mild coat defect. *Mol. Cell. Biol.* **20**, 9331-9336.

Pennisi, D., Gardner, J., Chambers, D., Hosking, B., Peters, J., Muscat, G., Abbott, C. and Koopman, P. (2000b). Mutations in Sox18 underlie cardiovascular and hair follicle defects in ragged mice. *Nat. Genet.* **24**, 434-437.

Reddy, S., Andl, T., Bagasra, A., Lu, M. M., Epstein, D. J., Morrisey, E. E. and Millar, S. E. (2001). Characterization of Wnt gene expression in developing and postnatal hair follicles and identification of Wnt5a as a target of Sonic hedgehog in hair follicle morphogenesis. *Mech. Dev.* **107**, 69-82.

Rodero, M. P., Hodgson, S. S., Hollier, B., Combadiere, C. and Khosrotehrani, K. (2013). Reduced Il17a expression distinguishes a Ly6c(lo)MHCII(hi) macrophage population promoting wound healing. *J. Invest. Dermatol.* **133**, 783-792.

Slee, J. (1962b). Developmental morphology of the skin and hair follicles in normal and in 'ragged' mice. *J. Embryol. Exp. Morphol.* **10**, 507-529.

Vidal, V. P. I., Chaboissier, M.-C., Lützkendorf, S., Cotsarelis, G., Mill, P., Hui, C.-C., Ortonne, N., Ortonne, J.-P. and Schedl, A. (2005). Sox9 is essential for outer root sheath differentiation and the formation of the hair stem cell compartment. *Curr. Biol.* **15**, 1340-1351.

Woo, W.-M., Zhen, H. H. and Oro, A. E. (2012). Shh maintains dermal papilla identity and hair morphogenesis via a Noggin-Shh regulatory loop. *Genes Dev.* **26**, 1235-1246.

Youssef, K. K., Lapouge, G., Bouvrée, K., Rorive, S., Brohée, S., Appelstein, O., Larsimont, J.-C., Sukumaran, V., Van de Sande, B., Pucci, D. et al. (2012). Adult interfollicular tumour-initiating cells are reprogrammed into an embryonic hair follicle progenitor-like fate during basal cell carcinoma initiation. *Nat. Cell Biol.* **14**, 1282-1294.

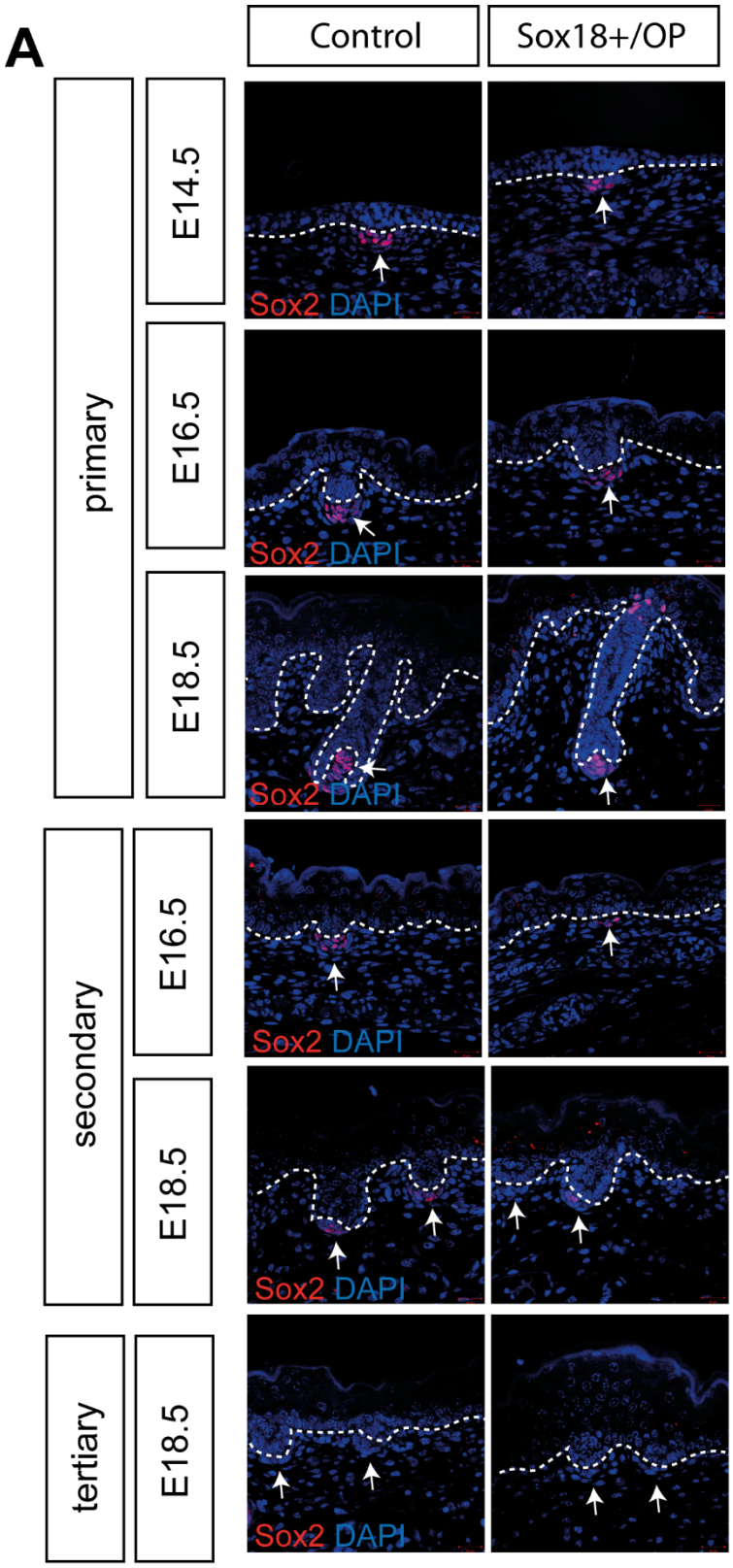

Supplemental Figure 1 : Primary and secondary hair DP development can be identified by Sox2 staining in control and Sox18$^{-/Op}$ skin. A) SOX2 (red) expression can be seen in early development of the primary hair follicle DP in both control and Sox18$^{-/Op}$ skin, at E14.5, E16.5 and E18.5 and in the developing secondary follicle at E16.5 and E18.5. As expected, at E18.5 no SOX2 expression was observed in the developing tertiary hair follicle DPs (arrows). All panels are counterstained with DAPI (blue), epidermal-dermal boundary indicated by dashed line, DP indicated by arrow.

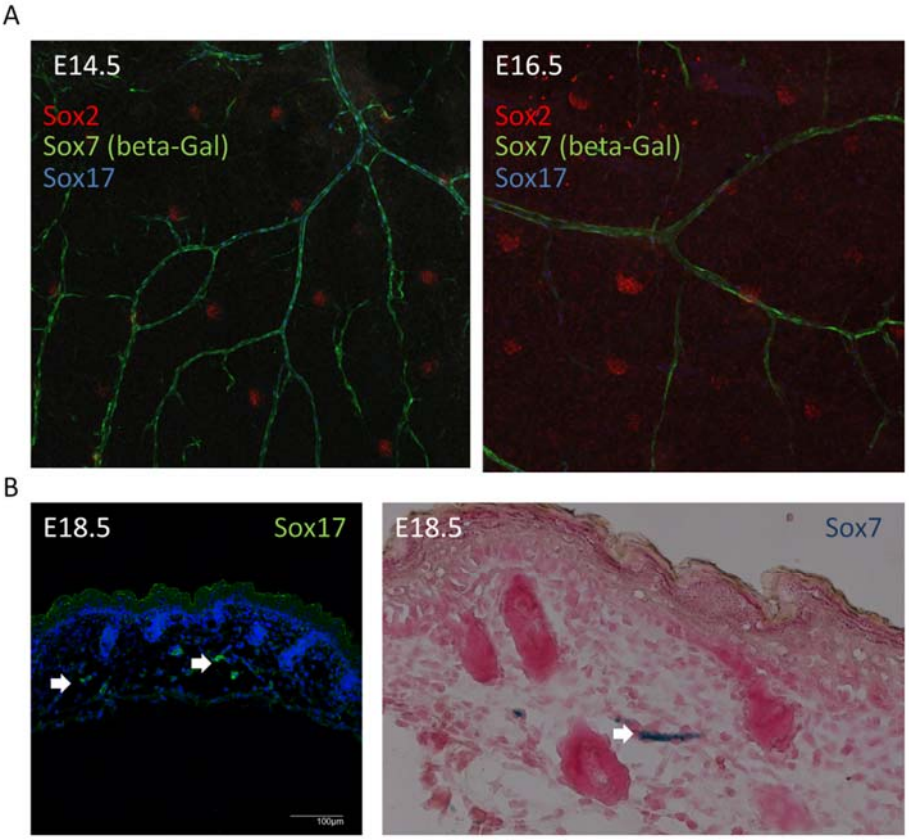

Supplemental Figure 2: *Sox18* expression in the dermal condensate is not associated with the expression of Sox7 and Sox17. A and B) Sox7-LacZ reporter mice were sacrificed at E14.5, E16.5 and E18.5. A) Whole mount Immunofluorescence of beta-galactosidase revealing Sox7 expression (green-cytoplasmic) combined with SOX17 (blue, nuclear) did not colocalize with dermal clusters as revealed by SOX2 (red) staining at E14.5 and E16.5. Sox7 and Sox17 could be visualized in vascular structures expectedly. B) At E18.5, sections were stained for SOX17 using immunofluorescence or histochemically stained with X-gal to reveal Sox7 related beta-galactosidase activity (blue) and counterstained with fast red.

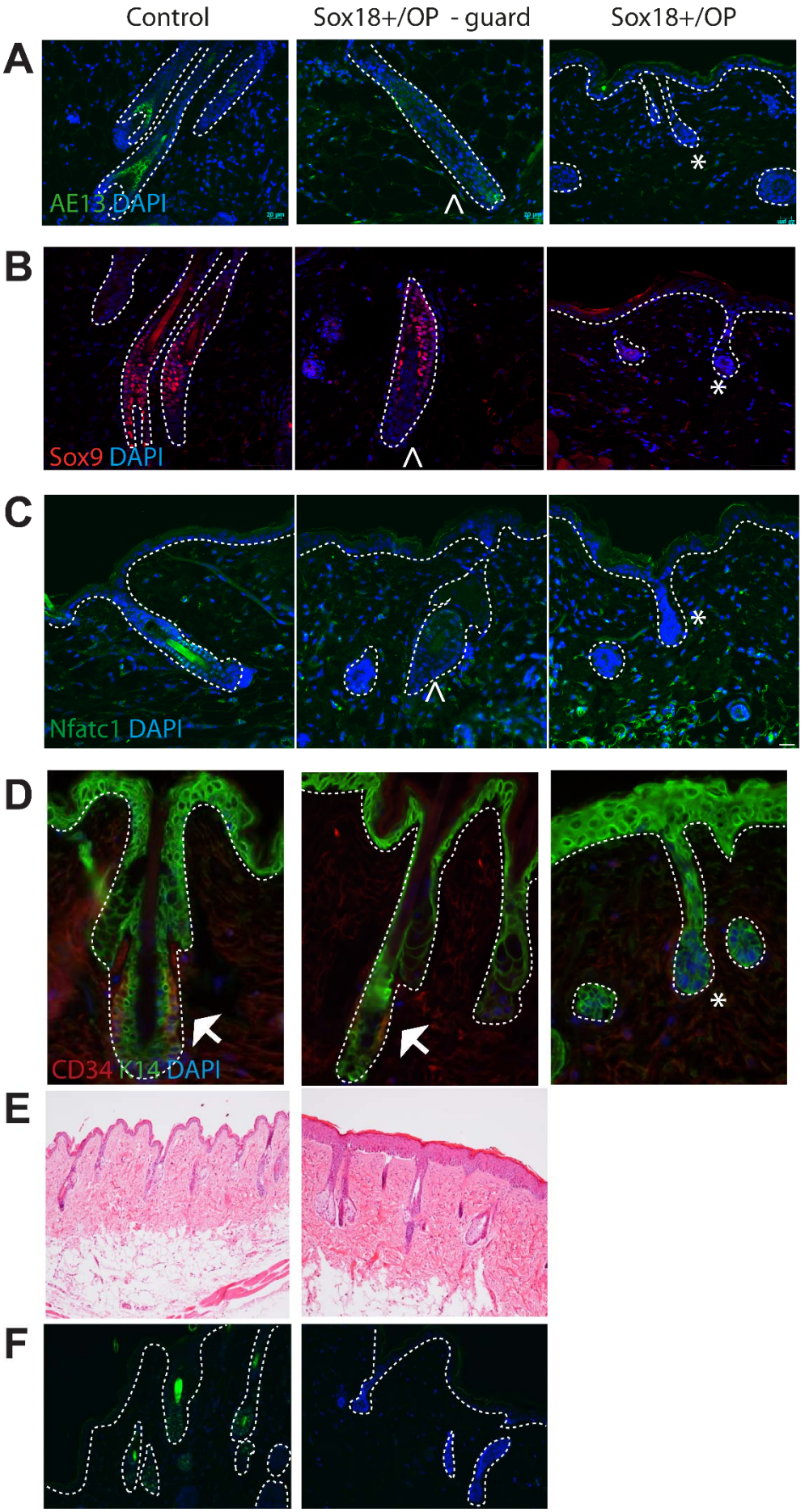

Supplemental Figure 3. Decreased hair differentiation and lack of stem cell quiescence in guard hairs in *Sox18$^{+/OP}$* mice. A) AE13 (green) in P24 control and *Sox18$^{+/OP}$* (RaOP) skin, guard (^) and non-guard hair remnants (*) indicated on panel. B) Sox9 (red) in P24 skin control, *Sox18$^{+/OP}$* guard (^) and non-guard hair remnants (*) indicated on panel. C) Nfatc1 (green) in P22 skin control, *Sox18$^{+/OP}$* guard (^) and non-guard hair remnants (*) indicated on panel. D) CD34 (red) and K14 (green) in P24 skin control, *Sox18$^{+/OP}$* guard and non-guard hair remnants, white arrows indicate regions of CD34/Keratin14 co-staining. E-F) WT and RaOP skin at 1 year of age. E) Haematoxylin and eosin stain, F) Sox9 staining (green) A), B), C), D) and F) counterstained with DAPI (blue), epidermal-dermal boundary indicated by dashed line.

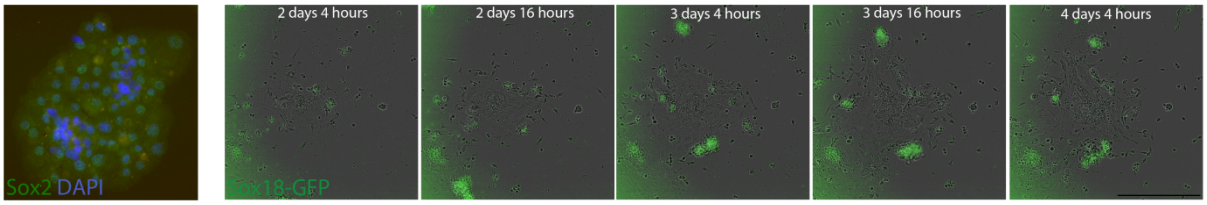

Supplemental Figure 4. Skin derived precursors (SKPs) isolated from neonatal dermis express Sox2 and Sox18. Left panel) Neonatal SKPs generated from wild-type mice were stained for SOX2 (green) and counterstained with DAPI (blue). (Other panels) Live imaging of neonatal SKPs generated from *Sox18*$^{+/GCre}$ mice showing GFP expression in forming spheres over time after culture (as indicated on each panel).

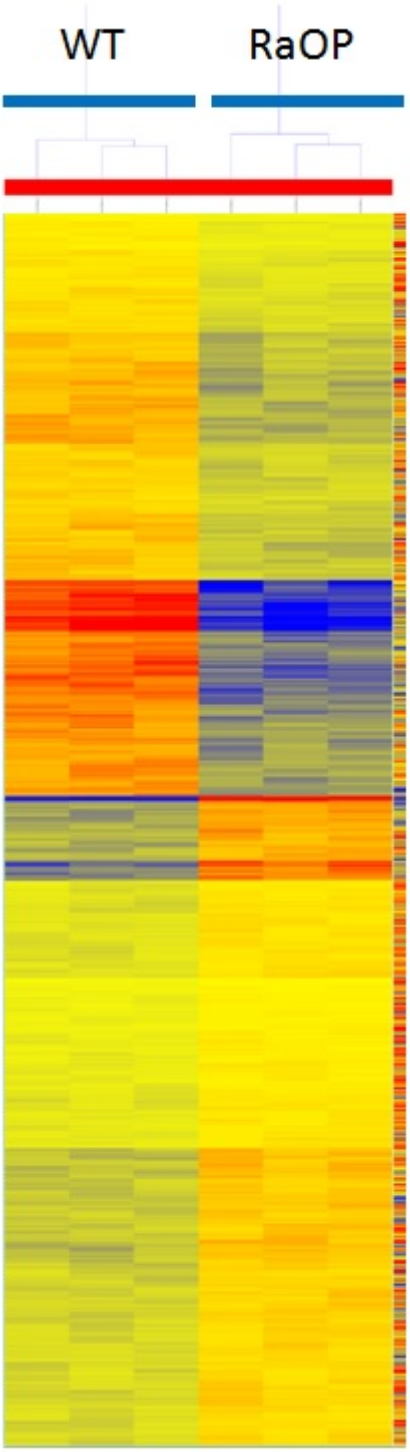

Supplemental Figure 5. Unsupervised hierarchical clustering of WT and Sox18+/OP SKPs. Gene expression analysis of Sox18+/OP (RaOP) and WT SKP spheres derived from littermates matched for sex allowed clear clustering of mutant and control mice.

Supplemental methods: Biotin labeled cRNA was produced using the Illumina® TotalPrep™ RNA Amplification (Ambion) as per supplier protocol. 50ng of starting total RNA was used and a 14 hour IVT reaction. cRNA samples was hybridized to Sentrix illumina_MouseWG-6 v2.0 Expression BeadChip overnight for 18 hours at 58^{o}C then scanned on a BeadStation 500 System using Beadscan software Version 3.5.31. Raw data was then imported into GenomeStudioV2010.2 for bead summarization and quality control assessment. Raw data files were submitted to Gene Express (accession number E-MEXP-3189). For data analysis, raw probe intensity data were imported into GeneSpring GX 11 and subsequent normalisation and significance analysis to identify differentially expressed probes were performed according to the default parameters used in the Guided workflow as outlined in the table below (adapted from GeneSpring GX 11 manual).